A STUDY OF METHODS USED IN

MEASUREMENT AND ANALYSIS OF SEDIMENT LOADS IN STREAMS

REPORT JJ

MODEL-B SEDIMENT-CONCENTRATION GAGE: FACTORS INFLUENCING ITS READINGS AND A FORMULA FOR CORRECTING ITS ERRORS

1989

REPORT JJ--MODEL-B SEDIMENT-CONCENTRATION GAGE: FACTORS INFLUENCING ITS READINGS AND A FORMULA FOR CORRECTING ITS ERRORS

A Study of Methods Used in

MEASUREMENT AND ANALYSIS OF SEDIMENT LOADS IN STREAMS

A Cooperative Project

Sponsored by the

Interagency Advisory Committee on Water Data

Subcommittee on Sedimentation

Participating Agencies

Corps of Engineers	**	Geological Survey
Forest Service	**	Bureau of Reclamation
Federal Highway Administration	**	Agricultural Research Service
Tennessee Valley Authority	**	Bureau of Land Management

REPORT JJ

MODEL-B SEDIMENT-CONCENTRATION GAGE: FACTORS INFLUENCING ITS READINGS AND A FORMULA FOR CORRECTING ITS ERRORS

By John V. Skinner

Prepared for Publication by the Staff of the
Federal Interagency Sedimentation Project
St. Anthony Falls Hydraulic Laboratory
Minneapolis, Minnesota

Published by
U.S. Army Engineer District
St. Paul, Minnesota

1989

Copies of this report are available from:

FEDERAL INTERAGENCY SEDIMENTATION PROJECT
ST. ANTHONY FALLS HYDRAULIC LABORATORY
HENNEPIN ISLAND & THIRD AVENUE S.E.
MINNEAPOLIS, MINNESOTA 55414

CONTENTS

ILLUSTRATIONS

TABLES

CONVERSION FACTORS AND ABBREVIATIONS

Readers who may prefer to use inch-pound units rather than the metric (International System) units used in this report can make conversions using the following factors:

Multiply metric unit	By	To obtain inch-pound
micrometer (μm)	3.937×10^{-5}	inch (in.)
millimeter (mm)	0.03937	inch (in.)
meter (m)	3.281	foot (ft)
milligram (mg)	3.527×10^{-5}	ounce, avoirdupois (oz)
gram (g)	0.03527	ounce, avoirdupois (oz)
liter (L)	1.057	quart (qt)
Liter (L)	0.2642	gallon (gal)
degree Celsius (°C)	°F = 1.8 x °C + 32	degree Fahrenheit (°F)

Other abbreviations used in this report

Abbreviation	Unit
μs	microsecond
s	second
min	minute
h	hour
μF	microfarad
μS	microsiemens

MODEL-B SEDIMENT-CONCENTRATION GAGE: FACTORS INFLUENCING ITS READINGS AND A FORMULA FOR CORRECTING ITS ERRORS

By John V. Skinner

ABSTRACT

A gage for measuring suspended-sediment concentration in flowing water was designed and tested. The gage contains a stationary, upstream-facing nozzle that guides a filament of the flow into a straight, slender tube. The tube vibrates continuously under control of magnets, coils, and electronic feedback circuits. A streamlined, waterproof shell serves as a protective housing for the tube and electronic components.

The measuring principle is based on two relations: one linking sediment concentration to slurry density, and the other linking slurry density to vibrational period. As sediment concentration increases, the slurry density increases, and this, in turn, causes the tube's vibrational period to increase.

Period readings can be converted to sediment-concentration values by using a calibration chart or an equation, but the first step is to minimize errors in the readings. Errors originate with (1) shifts in dissolved-solids concentration, (2) water temperature, (3) water pressure, (4) flow rate, and (5) the amount of debris on the tube's walls. Of these five factors, the first three directly influence slurry density. Water temperature and water pressure also influence vibrational periods by altering the tube's diameter. In certain situations, water temperature influences period readings by stretching or compressing the tube along its length. Flow rate exerts a mild influence on periods by creating Coriolis forces that press on the tube's walls. Debris on the walls alters period readings by changing the mass of the vibrating system.

An equation for correcting the first four errors is presented, and an example of the data-reduction format is given. Unfortunately, values of coefficients in the equation can be obtained only by installing a recording thermometer, a specific conductance meter, a staff gage, and a current meter. The thermometer must be exceptionally accurate and stable because the model-B gage is very sensitive to temperature shifts. Equipment for automatically removing debris from the tube walls is pictured and discussed in the report.

INTRODUCTION

Collecting records of suspended-sediment concentrations at remote river-gaging stations is a laborious and expensive process. Field personnel not only travel long distances to reach the stations; they also carry samplers, hoists, and crates of sample containers. After the water samples have been collected, the tedious analysis work begins. Because most samples contain only small quantities of sediment--typically less than a few grams per liter

of water--the laboratory work must be performed in an exacting manner. First, each sample is chemically treated to remove organic material. Then the sediment is extracted by filtering, centrifuging, or gravity settling. Finally, the sediment is dried at controlled temperatures, cooled in a humidity-free chamber, and then weighed on a sensitive laboratory balance.

The mutable nature of rivers complicates the task of collecting continuous, long-term sediment records. Most of the sediment discharged annually moves during high-runoff events lasting only a few hours or, at most, a few days. Important flow and concentration data are frequently lost because the events occur unexpectedly or during nighttime hours.

In 1984, the Sedimentation Project field-tested an instrument for automatically collecting sediment-concentration data. A submersible pump forced water through a U-shaped tube mounted on the river bank. The tube vibrated continuously and shifted its vibrational period with changes in sediment concentration. Every 5 minutes, readings of vibrational period, specific conductance of water, and temperature of water were collected. Then every 4 hours, readings were transmitted by telephone to a central computer that reduced the data and printed sediment-concentration values.

The instrument's accuracy was controlled mainly by water temperature. When temperatures remained stable, errors in concentration measurements were usually less than $\pm$ 25 mg/L (milligrams per liter); unfortunately, when temperatures fluctuated rapidly, the errors became larger. The growth in errors apparently stemmed from temporal lags in the instrument's thermal response. A sudden shift in temperature produced a slow shift in period. During the stabilization interval, which lasted about 20 minutes, measured sediment concentrations and computed sediment concentrations correlated poorly with one another.

In 1986, the Sedimentation Project built a new instrument termed the model-B sediment-concentration gage. Compared to the U-tube instrument, the model-B has two advantages: (1) it responds quickly to temperature shifts and consequently has a shorter stabilization interval, and (2) it can be submerged directly in river water and therefore operates without a sampling pump. Unfortunately, the model-B has not been field-tested. Problems likely to arise in field applications remain to be studied.

Purpose and Scope

This report (1) describes mechanical, electrical, and hydraulic features of the model-B sediment-concentration gage, (2) explains its mode of operation, (3) discusses factors influencing its readings, and (4) presents a formula for correcting its measurement errors.

The scope of this report is limited to the analysis of data collected in laboratory tests and in one simulated field test run in a laboratory supply channel connected to the Mississippi River.

Acknowledgments

Don Benson, U.S. Army Corps of Engineers (COE), arranged for casting, welding, and machining mechanical parts in the gage; LuVerne Fanjoy, COE, made the final mechanical adjustments. The author wishes to thank these individuals for their cooperation and technical assistance.

DESCRIPTION OF THE MODEL-B GAGE

The gage (fig. 1A) consists of four major parts: nozzle, tube, vibrator, and sleeve. The nozzle, which is stationary and faces upstream, guides a filament of the approaching slurry into the tube. The tube, which is the sensing element of the gage, vibrates at a period set by the density of the slurry. The tube has a diameter of 25.40 mm (millimeters) and was chosen because of its thin walls--they are only 0.51 mm thick. The low weight makes the tube sensitive to even slight changes in slurry density. The tube discharges the slurry behind the deflector fastened to the downstream end of the sleeve. The vibrator exerts a sinusoidal force on the tube and thereby sustains its oscillatory motion. The sleeve protects the tube and vibrator and also holds the ends of the tube stationary.

Details of the vibrator are shown in figure 1B. The magnet ring, which is a lightweight plastic band, grips the tube and also supports a pair of rod-shaped magnets that protrude into electric coils--one labeled "sense coil" and the other labeled "drive coil." The pipe plugs provide access to the coils and magnets.

Details of the nose assembly are shown in figure 1C. The nose itself is a bronze casting that streamlines the gage, supports the nozzle, and protects the tube lock and O-ring assembly.

The tube lock (fig. 1D) consists of (1) two concentric steel bands, (2) two cone-shaped rings, and (3) six bolts, two of which are shown in the sketch. As the bolts are tightened, the rings move toward one another and cause the outer band to expand against the sleeve and the inner band to contract around the tube. During assembly, a special adhesive is injected around the bands to cement them to the tube and sleeve. Near the tube lock, a pair of O-rings (fig. 1C) prevent helium gas inside the sleeve from leaking out and water outside the sleeve from leaking in.

The rear of the sleeve holds another tube lock, another pair of O-rings, a gas valve, the deflector, and an electrical plug. The gas valve forms a passageway for pumping helium into the sleeve. The deflector, which is a thin metal plate, maintains high flow rates through the nozzle by creating a low-pressure region at the discharge end of the tube. The electrical plug carries power to circuits inside the sleeve and also transmits period signals to a suspension cable that supports the gage.

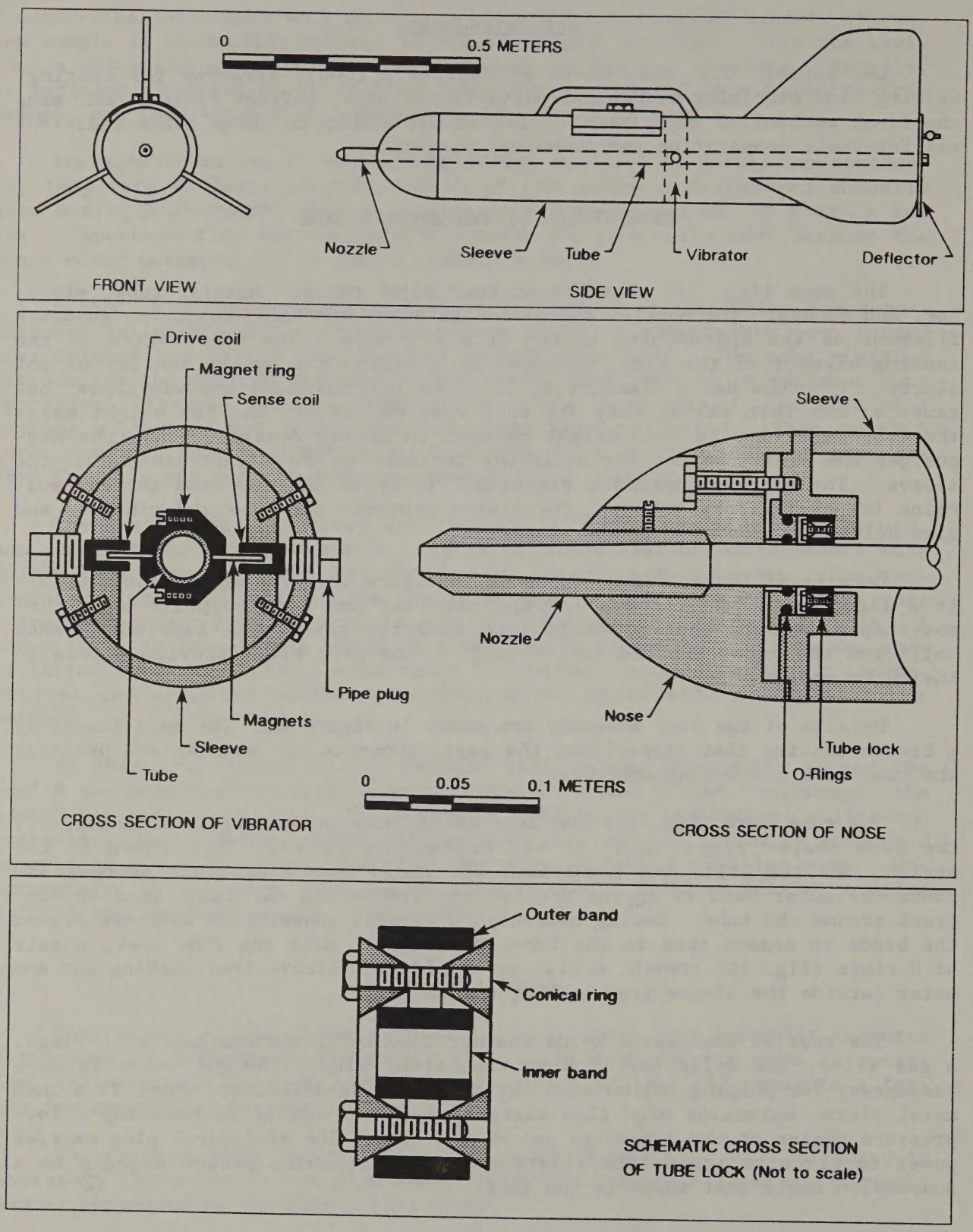

Figure 1.--Schematic showing the model-B sediment-concentration gage.

The gage's electrical circuits (see fig. 2) consist of three major sections: oscillator, suspension cable, and detector. The oscillator, which is mounted on a board inside the sleeve, forms a feedback circuit linking the sense coil to the drive coil. Movement of the tube generates a voltage in the sense coil. Then the multiplier A2, along with amplifiers A1, A3, and A4, amplifies the voltage and forces electric current through the drive coil. This current produces a magnetic field that alternately pushes and pulls on the magnet and reinforces the tube's motion.

Amplifier A5 stabilizes the drive-coil current. This amplifier has two inputs--one connected to the reference voltage and the other to the RMS to DC converter, which samples the drive-coil voltage. If the drive-coil voltage rises above a preset level, amplifier A5 decreases the gain of A2. Conversely, if the drive-coil voltage falls below a preset level, A5 increases the gain.

The suspension cable (1) supports the gage, (2) carries period signals from the gage up to a boat or bridge deck, and (3) carries battery current from a boat down to the gage. Inductors, one at each end of the cable, control the bidirectional flow of battery current and period signals. Battery current, which is steady, flows through the inductors and enters the DC-to-DC converter; however, period signals, which are unsteady and consist of sharp pulses, are blocked by the inductors and shunted into the detector circuit. A DC-to-DC converter transforms direct-current power from one voltage level to another. The converter in figure 2 transforms power from 24 volts to power at 15 volts.

Inside the detector circuit, period signals are amplified and then transmitted to the frequency meter shown in figure 2. Each component in the detector plays a role in this process. The resistor-capacitor network carries period signals from the cable to the transistor that performs the amplification. The 0.1 microfarad capacitor, which is connected to terminal "S," blocks the bias voltage produced by the transistor but passes the amplified signals on to the meter.

The frequency meter reads and displays either vibrational frequency or vibrational period. The choice is a matter of operator preference. Vibrational period in seconds is the quotient of 1.0 divided by the frequency in hertz. Throughout the remainder of this report, all readings will be cited as vibrational periods, and the units will be given in microseconds.

FACTORS INFLUENCING GAGE READINGS

Any measuring instrument reacts to several physical entities. One entity, termed the measurand, is the factor being sensed and displayed; the other entities, termed interferences, lead to uncertainties (errors) in the intended measurement. By way of example, consider a laboratory balance. The measurand is mass: the interferences are air currents around the pans, friction in the balance's pivots, and vibration of the workbench. Errors caused by the interferences can be almost eliminated by taking certain precautions--the pans can

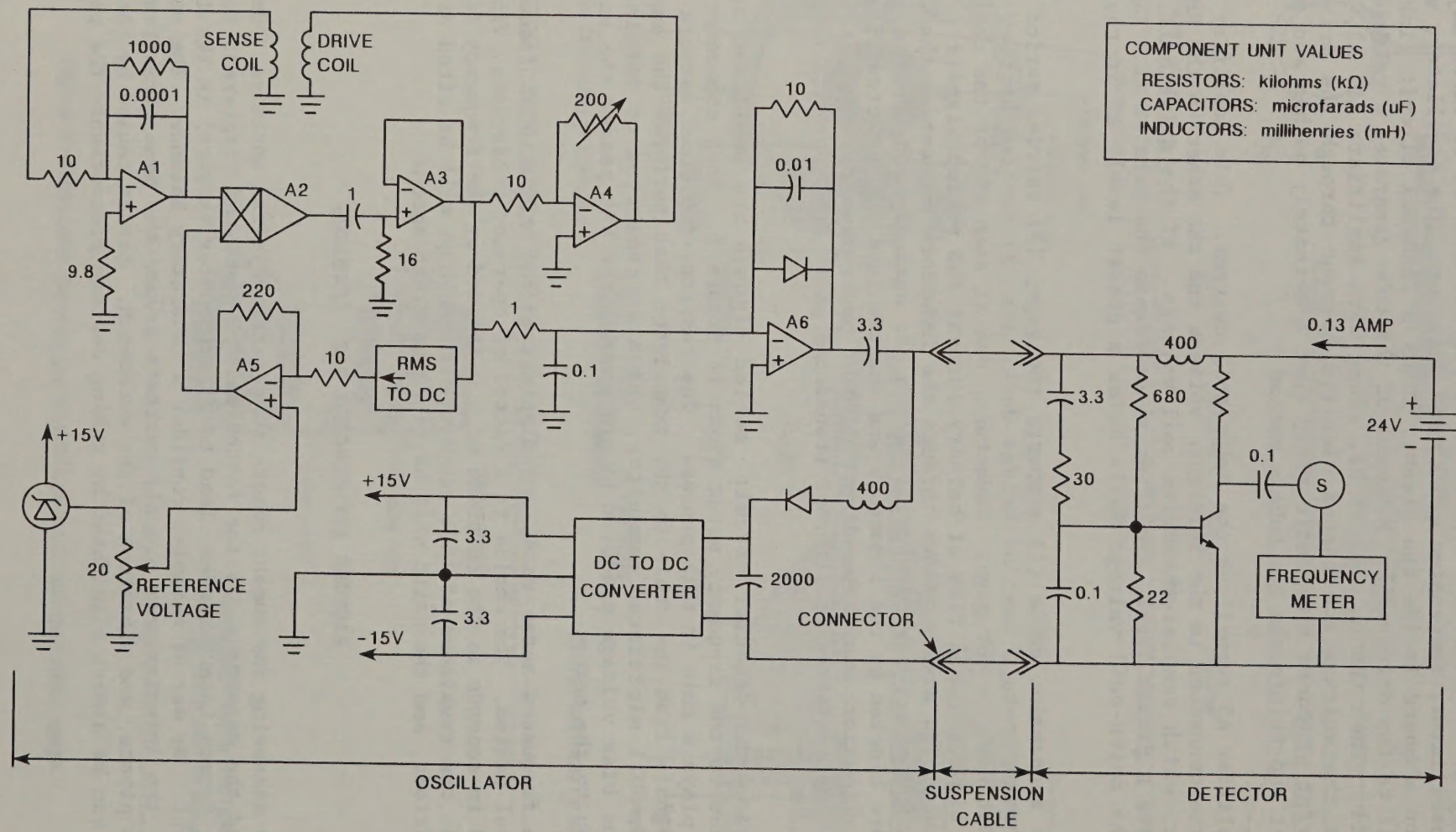

Figure 2.--Schematic of electrical wiring.

be shielded with airtight covers, the pivots can be cleaned and lubricated periodically, and the entire balance can be placed on vibration isolators. When all is done, mass readings are accurate and require no correction.

In some situations, interferences cannot be eliminated and correction factors must be applied. For example, consider a metal surveyor's tape. The measurand is length: interference stems mainly from air-temperature fluctuations. As the air warms and cools, the tape expands and contracts. Unable to control outside air temperatures, the surveyor must take temperature readings and then compute corrections based on the readings and the tape's thermal-expansion coefficient.

In one sense, the surveyor's tape is analogous to the model-B sediment gage--both instruments react to interferences that cannot be eliminated. In reducing sediment-gage data, we must follow the surveyor's lead by first measuring the interferences and then applying correction factors.

The remainder of this report discusses the gage's response to the measurand (sediment concentration) and to the interference factors. Coefficients developed in the discussions are incorporated into the error correcting scheme.

Suspended Sediment and Dissolved Solids

The first step in charting the gage's response to suspended sediment is selecting an appropriate calibration material. The Interagency Committee on Water Resources (1963) defines sediment as "fragmentary material that originates from weathering of rocks and is transported by, suspended, or deposited from water." Vanoni (1975) states that "although quartz, because of its great stability, is by far the commonest mineral found in sediment moved by water and wind, numerous other minerals are also present." He proceeds to cite mineralogical data on sand from the Missouri River at Omaha, Nebraska. Quartz comprised 49 percent of the material; other minerals (feldspar, carbonates, and chert) with densities nearly equal to that of quartz comprised another 28 percent. Bird and others (1963) examined principal fluvial-sediment minerals and found most have densities matching that of quartz. Since the sediment gage's response is strongly influenced by density, quartz seemed a logical choice for calibration.

The gage's response to water-quartz suspensions is plotted in figure 3. Notice that vibrational period increases as quartz concentration increases and that the trend line is almost straight. The particle-size distribution of the quartz test material is given in table 1.

River-born sediment particles come in a broad range of sizes, but fortunately particle size plays only a minor role in setting the gage's response. Szalona (1986) used an instrument similar to the model-B and conducted two tests--one on quartz particles in the silt-size range (4 to 62 μm (micrometers)) and the other on quartz particles in the fine-sand-size range (125 to 250 μm). Graphs of period readings plotted against sediment concentrations showed that trend lines for the two size ranges were nearly identical.

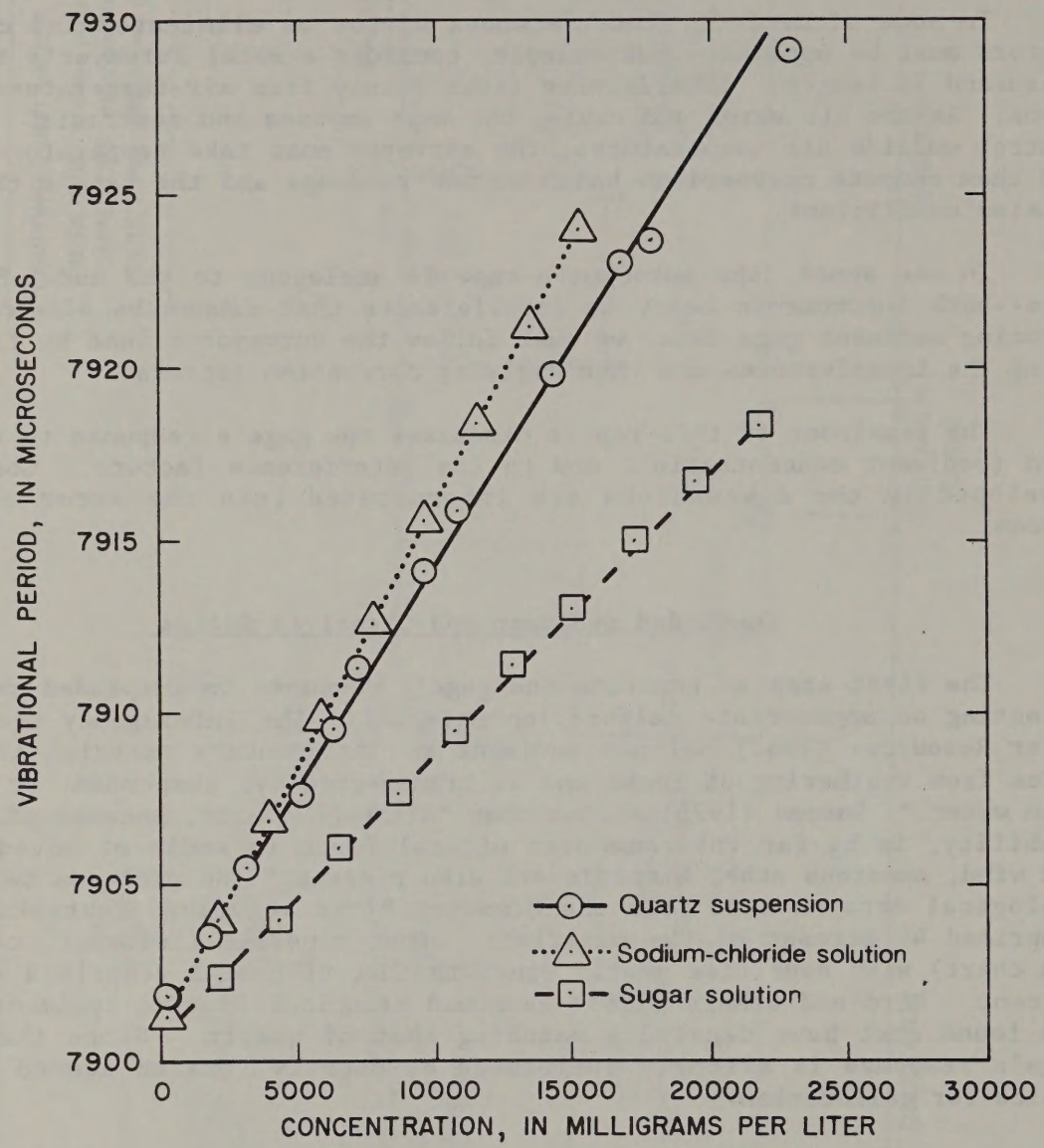

Figure 3.–Gage response to dissolved solids and suspended sediment.

Table 1.--*Particle-size distribution of quartz test sediment*

Particle diameter, in micrometers	Percent finer
149	100
125	97
105	91
88	60
62	14
44	7

Rivers transport biological particles that are lighter (less dense) than the mineral particles. This addition of lightweight material complicates the task of obtaining concentration values because the gage is sensitive to particle density (Skinner, 1982). Neutrally buoyant (lightweight) particles produce almost no shift in vibrational period; slightly heavier particles (for example, coal) produce small shifts; much heavier particles (for example, magnetite) produce large shifts. Vibrational-period readings must be interpreted carefully when flows contain high concentrations of organic material such as leaves, twigs, and algae.

In addition to particulate material, rivers contain a variety of dissolved solids. The gage's response to two compounds--sodium chloride and sugar--is plotted in figure 3. Notice that both trend lines are straight but that the sodium-chloride line is steeper than the sugar line. Sugar is rarely found in river water; however, the plotted data help illustrate that dissolved-solids composition can itself be a significant interference factor.

Specific conductance of water can be used to correct dissolved-solids interference. After surveying data on several rivers in the United States, Beverage (1982) found that a stable correlation between dissolved-solids concentration and specific conductance of water existed at many sites. He then installed a specific conductance meter and a commercially-manufactured vibrational gage on Willow Creek near Madison, Wisconsin. Data from the site indicated that the relation between vibrational period and dissolved-solids concentration was almost identical to the relation between vibrational period and suspended-sediment concentration (Skinner and others, 1986). This finding was not surprising because sodium chloride was used to melt ice on streets in the Willow Creek watershed, and the chemical was therefore a major dissolved-solids constituent in the flow. Figure 3 shows that for any given concentration, sodium chloride and quartz produce nearly equal vibrational periods.

Conclusions from the Willow Creek study can be used as a preliminary guide in interpreting information from other field stations. As a starting point, researchers may assume the slope of the dissolved-solids line matches the slope of the suspended-sediment line (see fig. 3). However, as more data become available, this assumption should be tested, and, if necessary, separate slope values should be evaluated by regression analysis.

Figure 4 illustrates a method for estimating dissolved-solids concentrations from specific-conductance-cell readings. First, linearity of the cell's output is checked by taking readings on several concentrations of sodium chloride dissolved in distilled water. Next, specific conductance readings are taken on one or more samples of river water from the site under investigation. Each sample is then filtered through a 0.45-μm filter to remove suspended particles. After evaporating the filtrate to dryness in a temperature-controlled oven, dissolved-solids concentration is computed by dividing the mass of the residue by the volume of filtrate. The specific conductance and concentration data for the sample are plotted. Then a straight line is drawn through the points and the intercept value for the probe (see "Mississippi River at Minneapolis, Minnesota" in fig. 4).

Before leaving the subject of suspended sediment and dissolved solids, let us examine an advantage of using sugar as a calibration material. The slope of the quartz-suspension line in figure 3 should be remeasured occasionally to disclose shifts in the gage's response; however, using quartz creates problems with wear and sampling in the test apparatus.

The test apparatus consists of a tank and a recirculating pump that are connected to form a closed loop with the vibrating tube in the sediment gage. When quartz is added to water in the loop, several things happen: (1) a few of the particles break up as they pass through the pump, (2) the pump's bearings begin to wear quickly, (3) some of the particles settle out of the flow, and (4) the remaining particles mix unevenly in the flow. Because concentration varies from point to point around the loop, flow emerging from the tube must be repeatedly sampled and analyzed to obtain concentrations within the tube itself. Substituting sugar for quartz eliminates not only the wear problem but also the need for sampling. Because sugar dissolves completely, concentration becomes uniform from point to point, and its value can be computed by dividing the mass of sugar added to the loop by the volume of water within the loop. When the sugar test is complete, the slope of the sugar-solution line can be multiplied by 1.63 to obtain the slope of the quartz-suspension line. Using sugar instead of salt for the calibration prevents the development of rust in the recirculating system.

Temperature

An abrupt shift in temperature produces a transition interval during which vibrational-period readings change according to certain patterns. As an example, figure 5A shows data from an experiment in which the sleeve is held at a steady temperature, while the tube and its contents (clear water) are cooled rapidly. As temperature drops, two opposing reactions develop. Water in the tube becomes denser, and this tends to slow the vibration and increase the vibrational period. At the same time, tensive forces appear in the tube's walls. Since the tube's ends are clamped (see fig. 1C), the tube reacts by pulling inward on the tube locks. The locks themselves respond by pulling outward on the tube. The stretching force decreases the tube's vibrational period much like tightening a violin string raises its pitch. The downward trend of the dotted line in figure 5A indicates that the stretching-force effect is stronger than the density-shift effect.

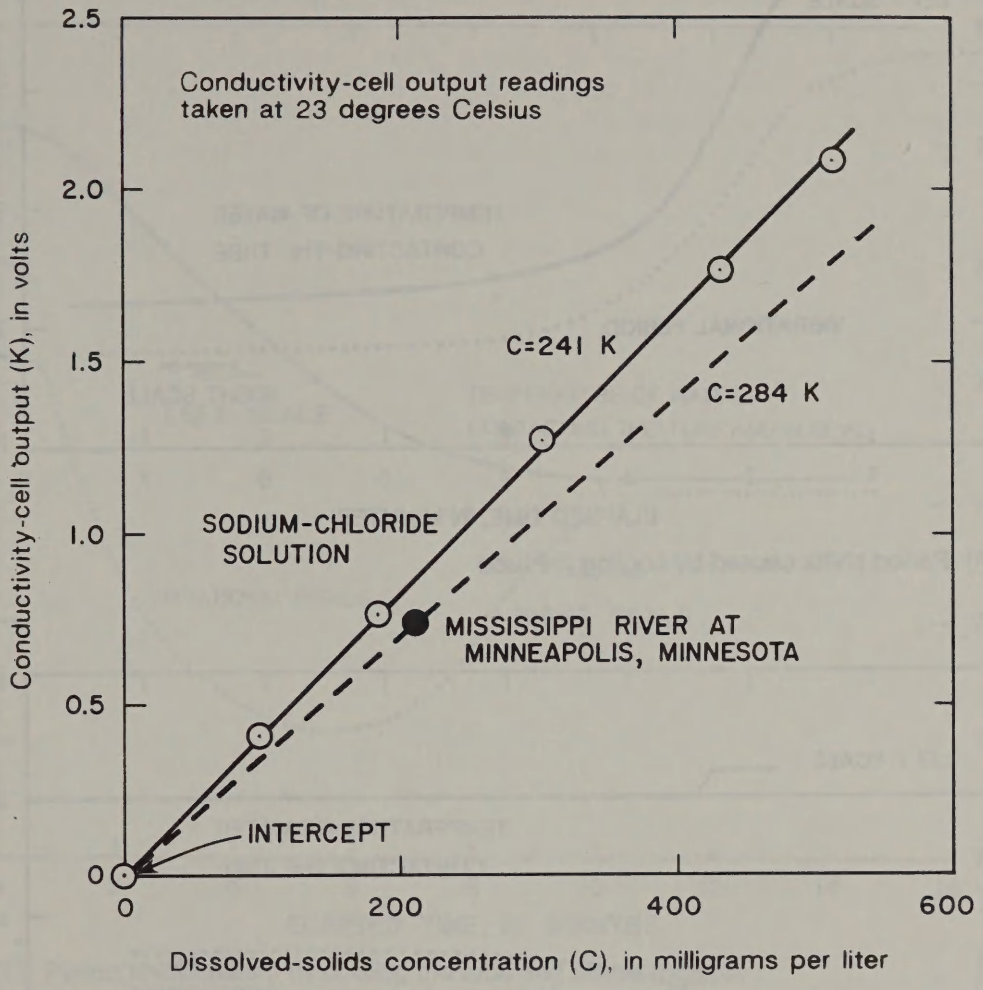

Figure 4.--Graphical method for estimating dissolved-solids concentration from specific conductance-cell output.

FIG 1

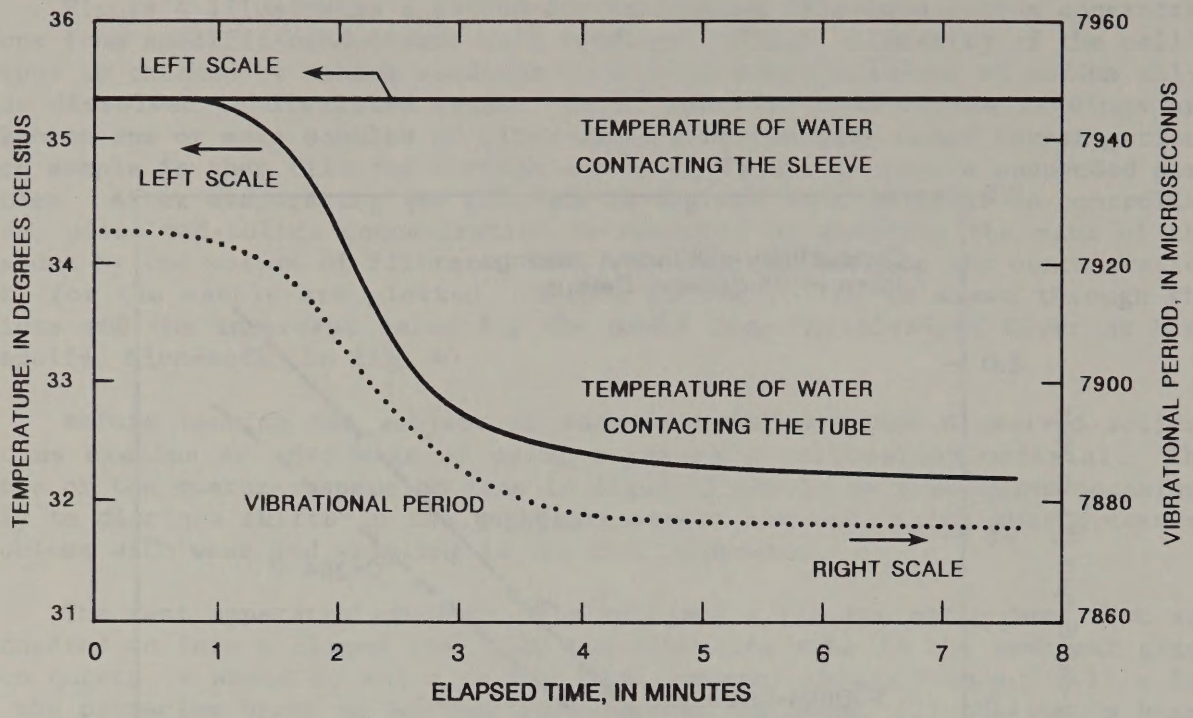

(A) Period shifts caused by cooling the tube

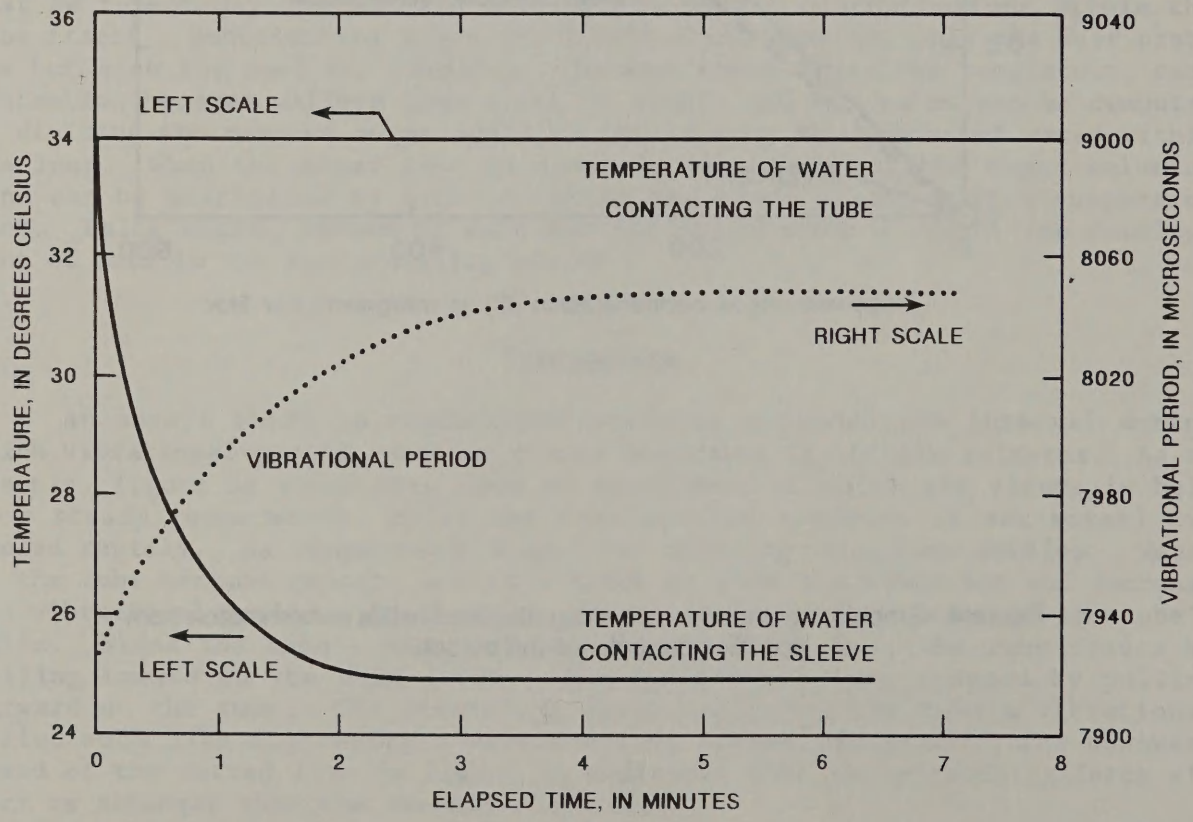

(B) Period shifts caused by cooling the sleeve

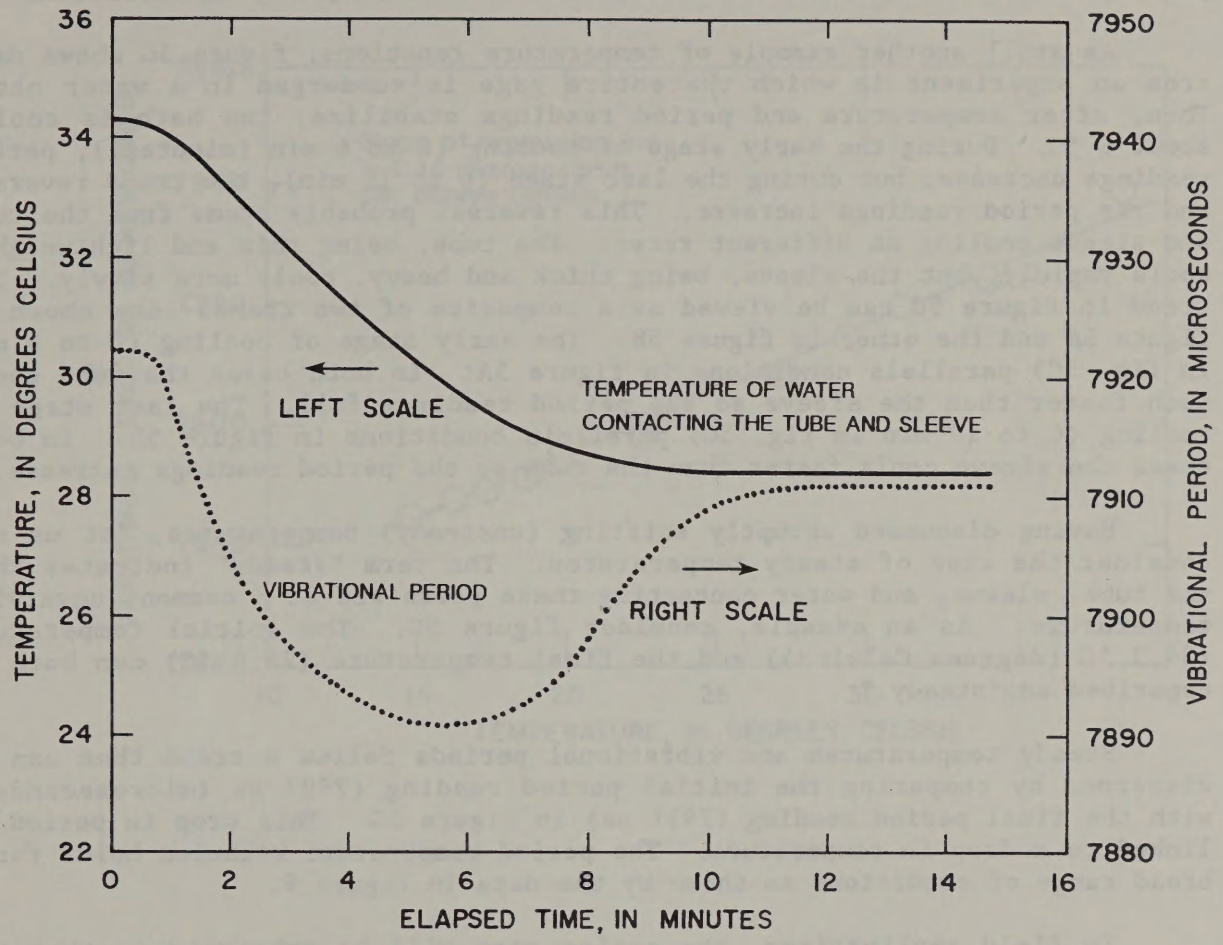

(C) Period shifts caused by cooling the tube and sleeve together

Figure 5.--Gage response to unsteady temperatures.

As another example of temperature reactions, figure 5B shows data from an experiment in which the tube and its contents (clear water) remain at a steady temperature while the sleeve cools rapidly. As it cools, the sleeve contracts and pulls the tube locks toward one another. The resulting compressive force increases the tube's vibrational period much like applying a compressive force to a slender rod lowers its natural frequency of vibration.

As still another example of temperature reactions, figure 5C shows data from an experiment in which the entire gage is submerged in a water bath. Then, after temperature and period readings stabilize, the bath is cooled about 6 °C. During the early stage of cooling (0 to 6 min (minutes)), period readings decrease; but during the last stage (6 to 11 min), the trend reverses and the period readings increase. This reversal probably stems from the tube and sleeve cooling at different rates. The tube, being thin and lightweight, cools rapidly, but the sleeve, being thick and heavy, cools more slowly. The trend in figure 5C can be viewed as a composite of two trends--one shown in figure 5A and the other in figure 5B. The early stage of cooling (0 to 6 min in fig. 5C) parallels conditions in figure 5A: in both cases the tube cools much faster then the sleeve so the period readings fall. The last stage of cooling (6 to 10 min in fig. 5C) parallels conditions in figure 5B: in both cases the sleeve cools faster than the tube so the period readings increase.

Having discussed abruptly shifting (unsteady) temperatures, let us now consider the case of steady temperatures. The term "steady" indicates that the tube, sleeve, and water contacting these parts are at a common, unvarying temperature. As an example, consider figure 5C. The initial temperature (34.3 °C (degrees Celsius)) and the final temperature (28.4 °C) can both be described as "steady."

Steady temperatures and vibrational periods follow a trend that can be discerned by comparing the initial period reading (7923 μs (microseconds)) with the final period reading (7911 μs) in figure 5C. This drop in period is linked to a drop in temperature. The period-temperature relation holds for a broad range of conditions as shown by the data in figure 6.

In field applications, the entire gage will be submerged so that the sleeve temperature and the tube temperature will both shift toward the river-water temperature. Furthermore, the period reading will lie on the trend line of figure 6 provided the river-water temperature either remains steady or shifts slower than a certain critical rate.

We can estimate the critical rate from data in figure 7. The top chart shows temperature readings taken with the gage submerged in a water bath. Numbers beside the trend line give rates of change in degrees per hour. The bottom chart (fig. 7) shows two forms of vibrational-period data. The solid line connects values obtained by transforming temperature readings on the top chart to vibrational-period readings by using the regression-relation readings in figure 6. The circles on the bottom chart (fig. 7) represent measured values obtained with a frequency meter. Disparity between the predicted and measured values is a key factor in determining the critical temperature rate. The ten points labeled "R" fall above the solid line and coincide with inter-intervals of rapid warming (see top chart, fig. 7). Evidently, warming rates

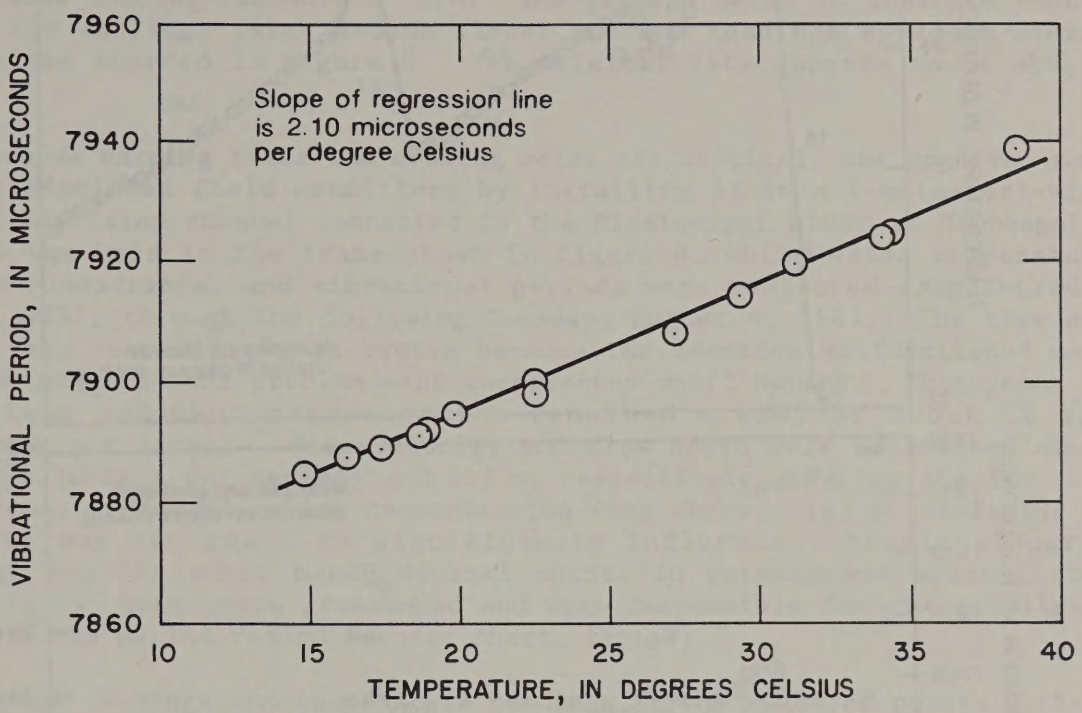

Figure 6.--Gage response to steady temperatures.

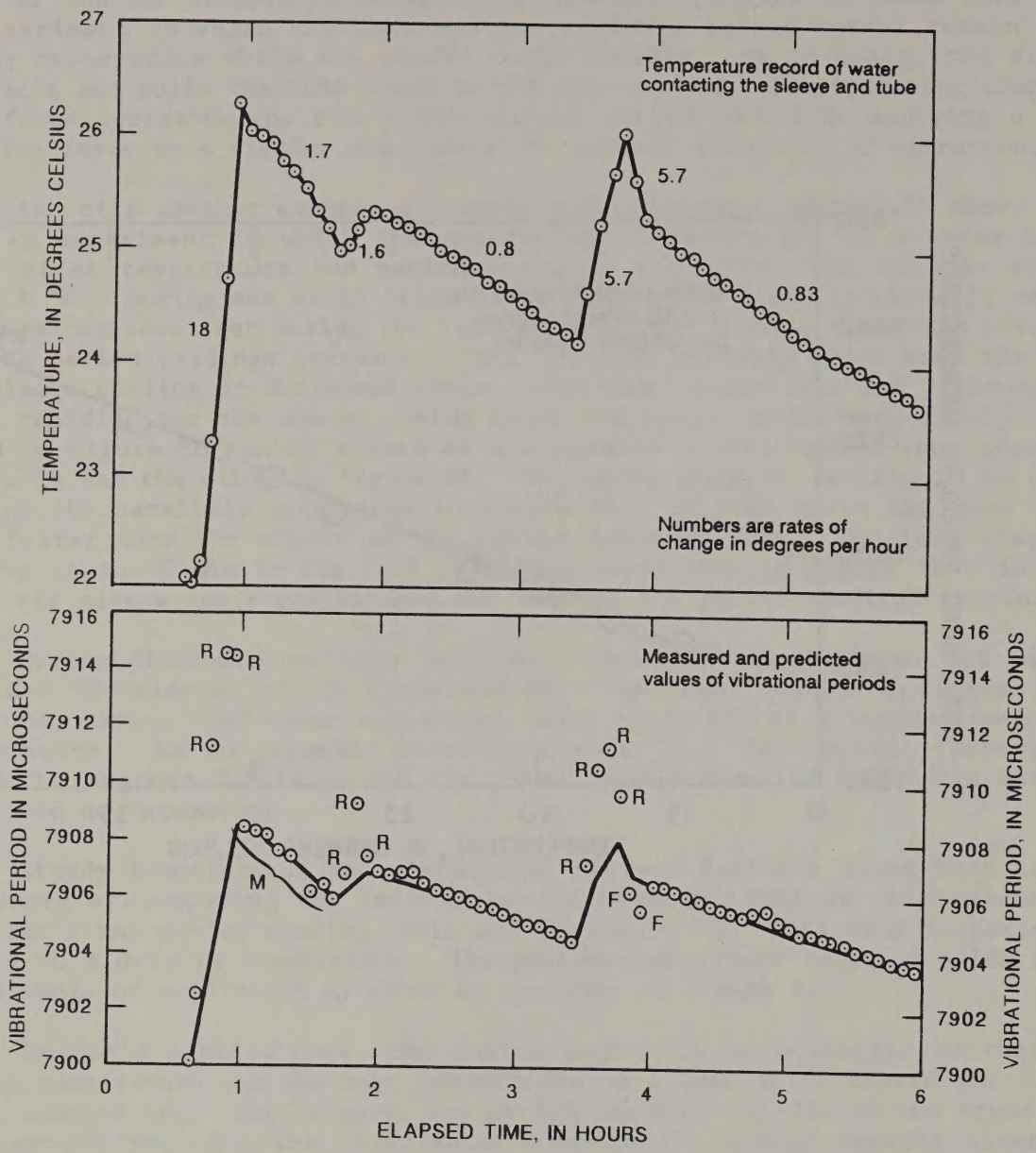

EXPLANATION

- Predicted vibrational periods based on gage response to steady temperatures
- O Measured periods
- R Measurements taken during rapid-warming trend (rates exceeding 1.5 degrees Celsius per hour)
- F Measurements taken following rapid-cooling trend (rates approximately 5.7 degrees Celsius per hour)
- M Measurements taken during moderately slow cooling trend (rates approximately 1.7 degrees Celsius per hour)

Figure 7.--Comparison of measured and predicted values of vibrational periods.

exceeding about 1.5 °C/h (degrees Celsius per hour) create instabilities. The two points labeled "F" fall below the line and immediately follow an interval of rapid cooling. Here again, rapid changes in temperature create instabilities. The eight points labeled "M" plot near the line and occur during a moderately slow cooling rate--only 1.7 °C/h. The unlabeled points (bottom chart, fig. 7) plot almost exactly atop the line and occur during intervals of extremely slow cooling--about 0.8 °C/h. The pattern seems to indicate that as warming (or cooling) rates become slower, period readings approach steady-state values charted in figure 6. The critical rate appears to be about 1 °C/h.

Because warming rates and cooling rates are critical, the gage was tested under simulated field conditions by installing it in a 1-m (meter)-wide, 2-m deep diversion channel connected to the Mississippi River at Minneapolis. The gage was held in the frame shown in figure 8, while water temperature, specific conductance, and vibrational periods were monitored from Thursday, July 30, 1987, through the following Tuesday, August 4, 1987. The time axis for the data (see fig. 9) is broken because the recorder malfunctioned early Sunday morning and the problem went uncorrected until Monday. Throughout the entire test sediment concentration remained steady at about 12 mg/L (milligrams per liter). Flow velocity and flow depth were maintained steady at 0.3 m/s (meters per second) and 1.7 m, respectively. During the last half of the test, dissolved-solids concentration (top chart, fig. 9) declined, but the shift was too small to significantly influence vibrational-period readings. On the other hand, diurnal shifts in water temperature (bottom chart, fig. 9) were quite pronounced and were responsible for the oscillating pattern in the period record (center chart, fig. 9).

Period readings and temperature readings at the numbered points (1-13) in figure 9 are plotted in figure 10. Comparing figure 10 with figure 6 shows that the regression lines have nearly equal slopes even though the lines are vertically displaced from one another. As an example of the displacement, consider readings at 30 °C; the period from figure 10 is 8077 μs, but the period from figure 6 is only 7918 μs. This difference probably stems from vibration of the sleeve. Even though the sleeve's amplitude of vibration is small, the motion makes the gage sensitive to acoustic reverberations in the surrounding water and in the supporting framework.

Pressure

Figure 11 shows that period readings increase slightly when the gage is lowered through the water. Disregarding readings taken at the water surface ("A" in fig. 11) and at the channel bottom ("B" in fig. 11), the gage's depth sensitivity is about 1 μs/m.

The sleeve vibrates slightly and radiates pressure waves into the surrounding water. These waves travel away from the gage until they strike a discontinuity that then acts like a mirror and reflects the waves back to their starting point.

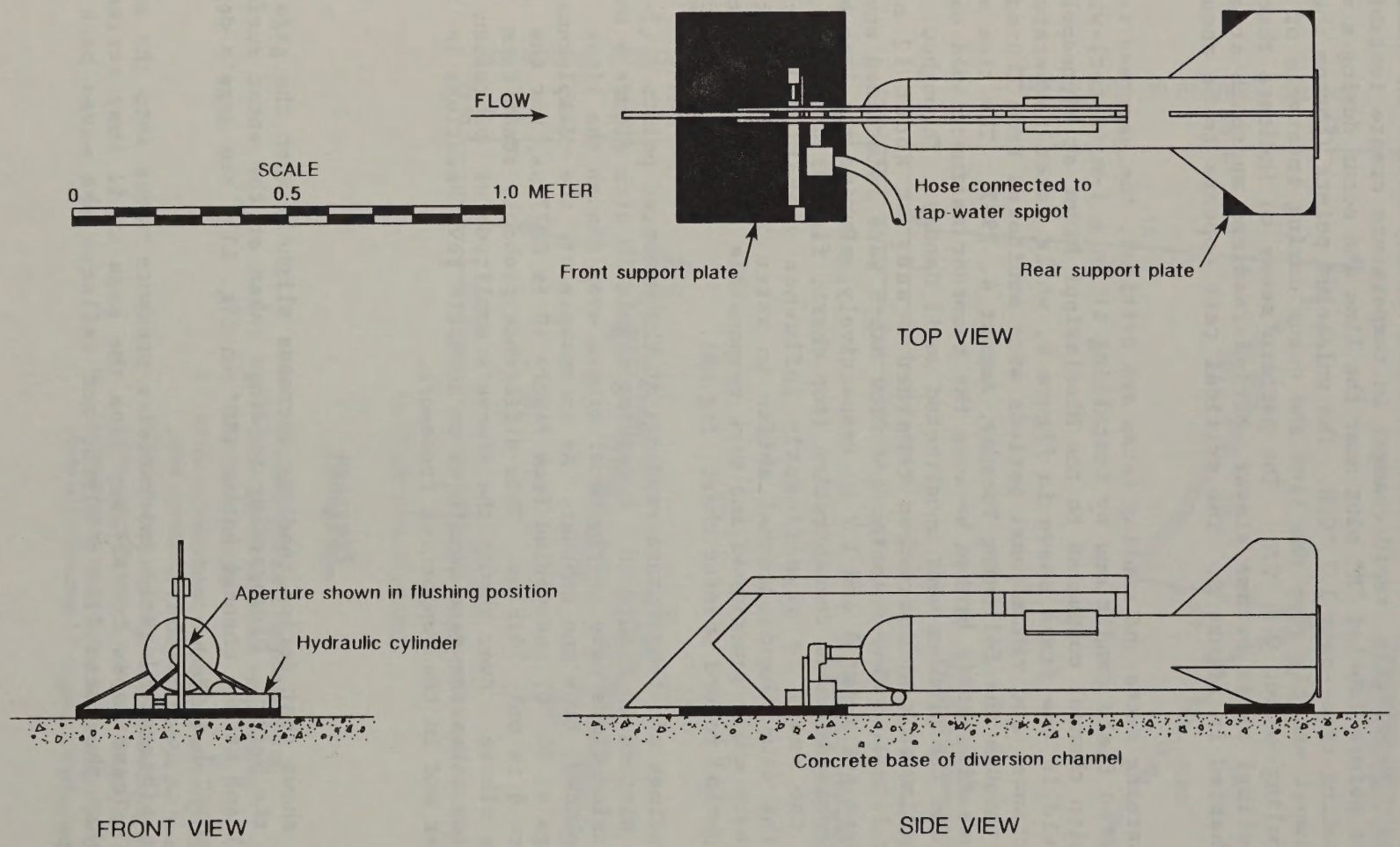

Figure 8.--Support frame for diversion-channel test.

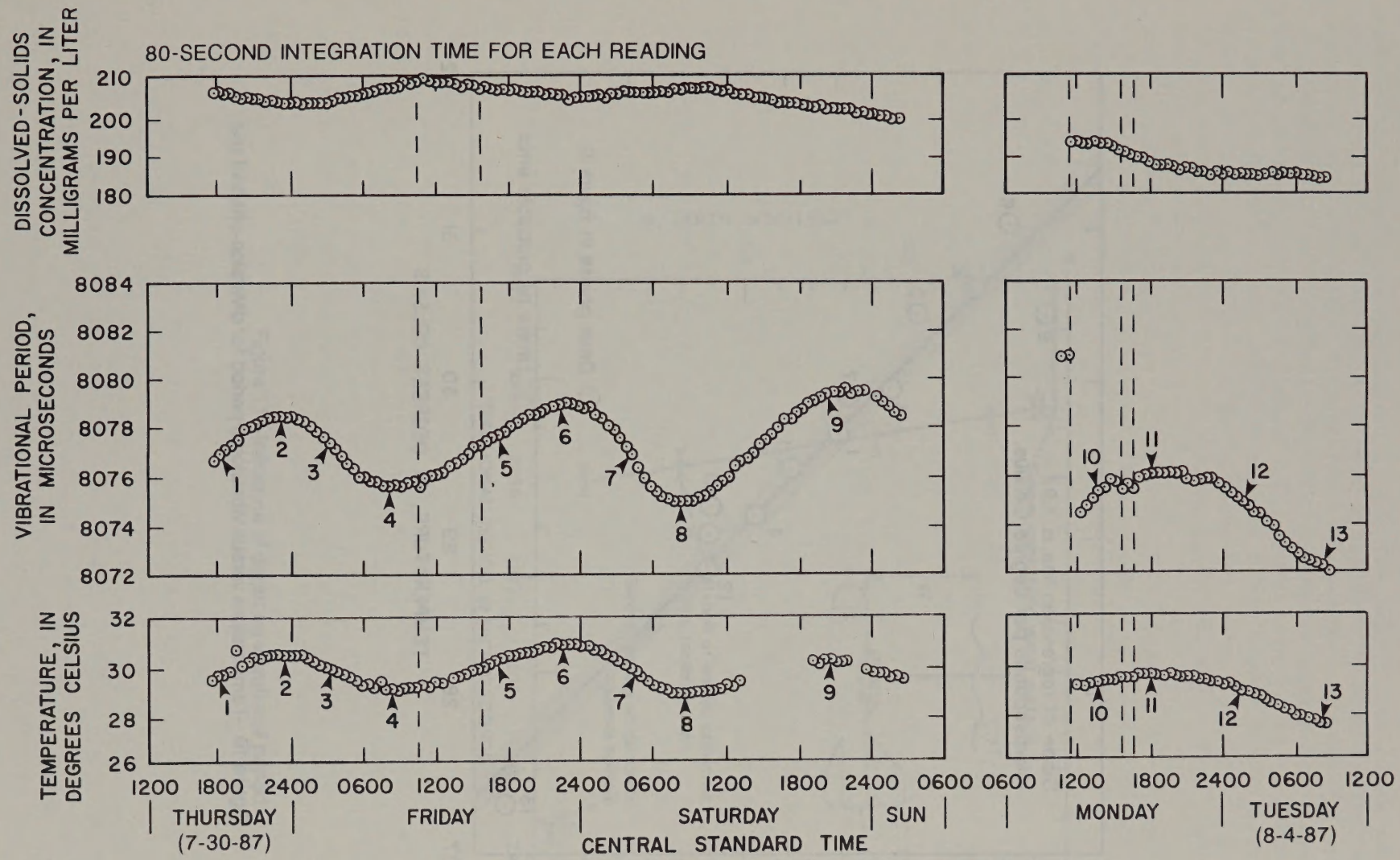

Figure 9.--Records of diversion-channel test.

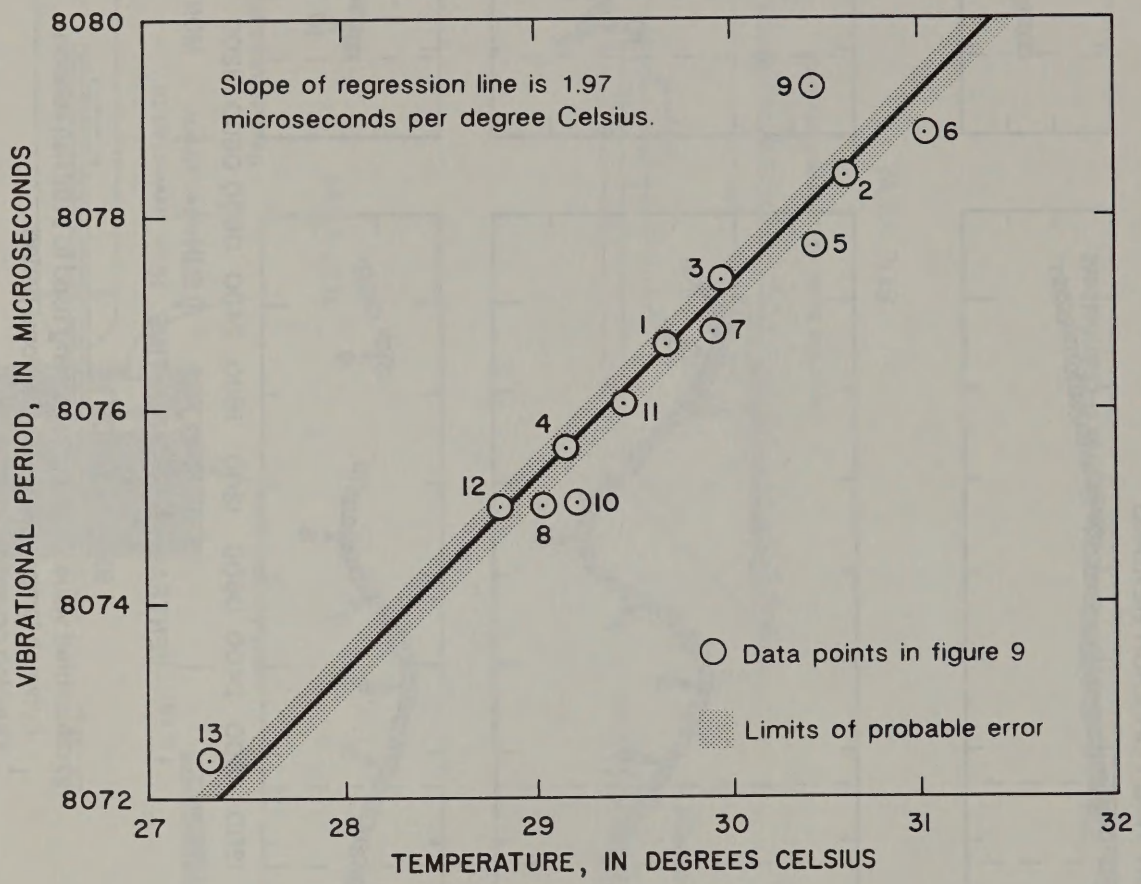

Figure 10.--Temperature versus vibrational period for diversion-channel test.

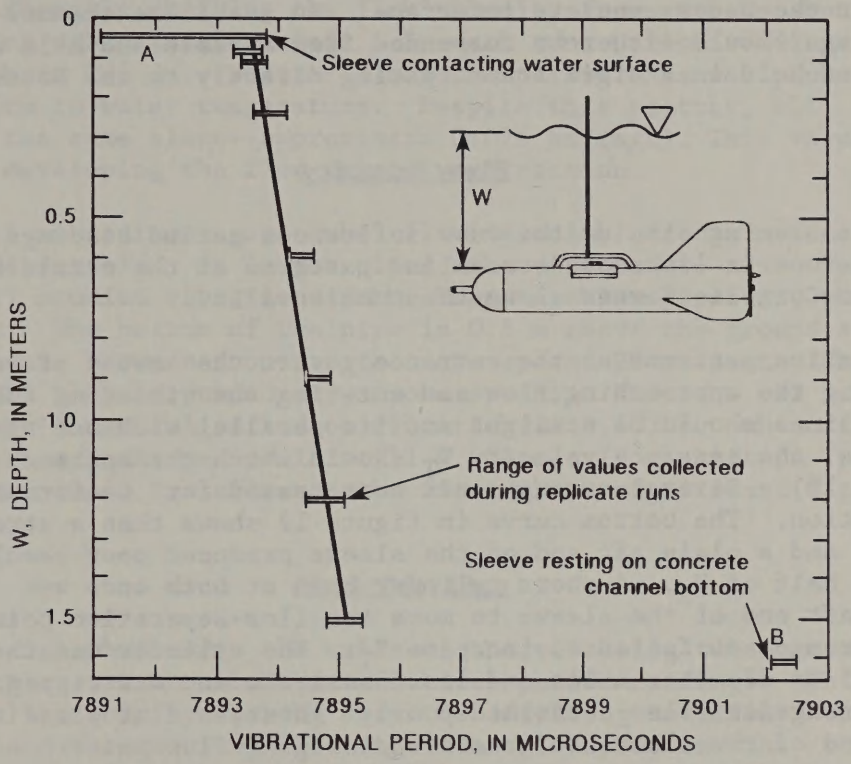

Figure 11.--Influence of depth on vibrational period.

The water-surface readings in figure 11 have a large variance that stems from (1) experimental errors in measuring the distance "W" to the sleeve and (2) discontinuities formed by the air-water interface. When the gage is near the surface, upward traveling waves combine with reflected, downward traveling waves to produce interference patterns. The intensity and distribution of the patterns are sensitive to even small ripples on the water surface. To minimize water-surface effects, period readings should be collected only when the gage is more than about 0.1 m below the surface.

The channel-bottom readings ("B" in fig. 11) have a small variance, but the points fall far to the right of the solid trend line. This abrupt shift occurs when the sleeve touches the channel bottom and the waves are strongly reflected at the water-concrete interface. To stabilize channel-bottom readings, the gage should either be suspended from a cable and held slightly above the bottom or held in a rigid frame resting directly on the bottom.

Flow Velocity

Water flowing inside the tube influences period readings through two mechanisms: one is linked to streamline patterns at the nozzle's entrance and the other to Coriolis forces along the tube's walls.

Streamline patterns at the entrance govern the amount of water and sediment leaving the approaching flow and entering the vibrating tube. Ideally, the streamlines should be straight and lie parallel with one another, or, in other words, the entrance velocity V_T should match the approach velocity V_A (see fig. 12). Several arrangements were tested for conformance with the ideal situation. The bottom curve in figure 12 shows that a straight hole in the nozzle and a plain aft end on the sleeve produced poor results: V_T was only about half of V_A. A short cylinder open at both ends was then clamped around the aft end of the sleeve to move the flow-separation point downstream, but this arrangement failed to increase V_T. The cylinder was then perforated with four 25-mm-diameter holes and its downstream end was capped. This side-venting arrangement also performed poorly. Next, a flat plate was bolted to the aft end of the sleeve to create a diverging flow pattern and lower the pressure at the exhaust end of the vibrating tube. The plate increased V_T, but the plate also increased drag forces on the gage. Additional tests indicated a smaller plate--one with a diameter of 254 mm--reduced the drag force without sacrificing improvements in V_T. As a final measure, a special taper-bore nozzle was built and installed in place of the straight-bore nozzle. V_T values with the tapered nozzle and flat-plate combination are plotted as circles in figure 12. The trend line falls slightly below the ideal, but the mismatch is not serious. The V_T/V_A ratio is about 0.95 through a broad range of approach velocities. Data collected by other investigators (Interagency Committee, 1941) indicate concentrations of sand-size particles inside the tube will be only 3 percent greater than concentrations of the particles in the approaching flow.

Let us now consider Coriolis forces inside the tube. As the tube oscillates, it moves back and forth between the solid curve and dotted curve in figure 13. For analysis purposes, the tube can be divided into small segments, one of which is shown by the darkened area. This segment not only translates up and down but it also rotates back and forth--first in a counter-

clockwise direction and then in a clockwise direction. Flow enters from the left at a steady velocity. At one instant the flow-velocity vector slopes downward, but a few milliseconds later the vector slopes upward (see V_1 and V_2 on fig. 13). The Coriolis acceleration vector, which is obtained by subtracting V_1 from V_2, is almost normal to the tube's axis and is colinear with the Coriolis force vector. A shift in this force vector causes a shift in wall pressure, which, in turn, causes a change in the tube's vibration period. Interference arises because the period shift appears to stem from a change in sediment concentration.

Figure 14 shows Coriolis effects in the 1-inch-diameter tube when it is filled with flowing tap water. The four lines in figure 14 are replications performed by abruptly shifting the flow velocity from zero to about 1.4 m/s while recording vibrational periods. In each run, period readings increased but only by about 0.1 μs. Scatter along the period axis was probably caused by small shifts in water temperature. Despite this scatter, all four lines have nearly the same slope--approximate 0.075 μs/(m/s). This value will be used later in developing the flow-velocity correction.

In the 25-mm sediment-gage tube, flow-velocity effects are so weak as to be almost undetectable. In larger pipes, the effects are also very feeble. Housner (1952) studied vibration in the Trans-Arabian pipeline, which is 760 mm in diameter. The bottom of the pipe is 0.5 m above the ground so the pipe is free to vibrate between supports that are spaced 20 m apart. The pipe carries crude oil that is pumped at various speeds. When the oil is standing still the pipe's natural period of vibration is 0.403 s, when the oil is flowing at 4.6 m/s the period is still 0.403 s. If a shift in period does occur, it is too small to influence the first three significant digits.

Wall Coatings

Any material that coats the walls of the vibrating tube becomes part of the oscillating system and thereby influences period readings. This influence can be controlled only by washing away the offending material. The rate of accumulation and the required cleaning interval depend on the concentration and type of contaminants in the flow. The water-bath tests discussed earlier were run with clean, chlorinated tap water, so wall-coating effects were never a problem; however, because the diversion-channel tests were run with algae-laden river water, wall-coating effects became quite severe. Warm temperatures fostered the growth of long strings of slime that hooked over the nozzle and streamed back into the tube. For cleansing purposes, the support frame was fitted with an aperture (see fig. 8) connected through a garden hose to a tap-water spigot. The cleaning operation involved three steps. First, the hydraulic cylinder was pressurized to swing the aperture in front of the sediment-gage nozzle. Second, the tap-water spigot was opened for several seconds to force a jet of clean water through the tube. Third, the hydraulic cylinder was pressurized again but this time to swing the aperture down and away from the nozzle.

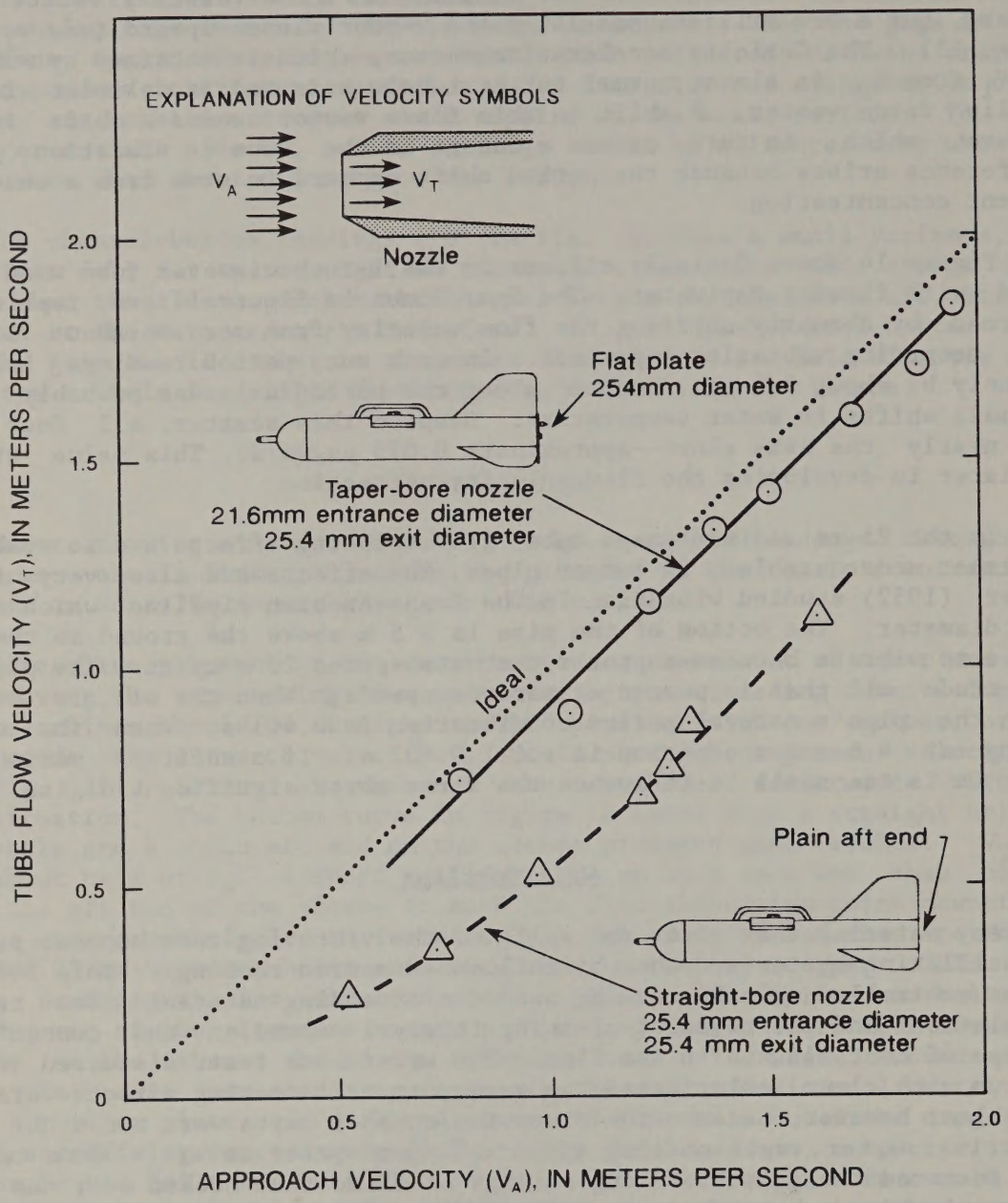

Figure 12.--Relation between approach velocity and tube-flow velocity.

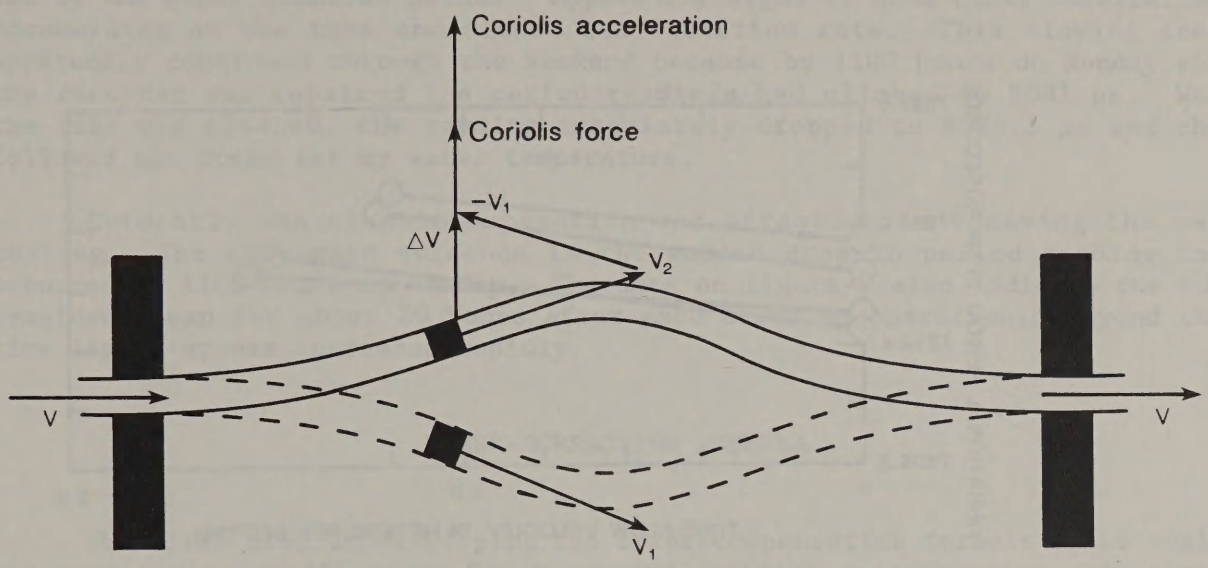

Figure 13.--Velocity, acceleration, and force vectors for a vibrating, liquid-filled tube.

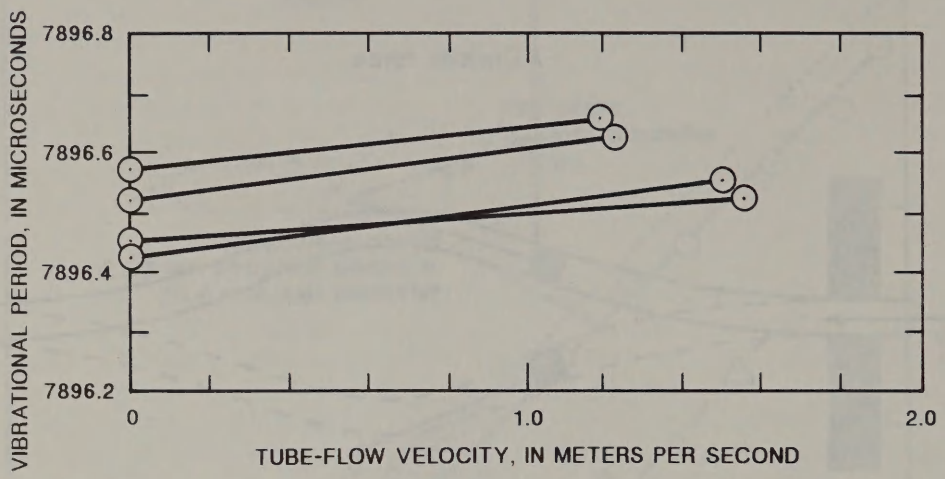

Figure 14.--Relation between tube-flow velocity and vibrational period.

Five cleaning operations are indicated by the dotted lines in figure 9. The first operation was performed on Friday at 1030 hours and the last was performed on the following Monday at 1630 hours. From 1530 hours on Friday until about 0800 hours on Saturday, period readings followed a pattern dictated by shifts in water temperature. However, at 2200 hours on Saturday, the period reading registered at an abnormally high value of 8079.5 μs. This reading, labeled "9" on figure 9 and on figure 10, falls above the trend line set by the other numbered points. Apparently algae or some other material had accumulated on the tube and slowed its vibration rate. This slowing trend apparently continued through the weekend because by 1100 hours on Monday when the recorder was repaired the period readings had climbed to 8081 μs. When the tube was cleaned, the reading immediately dropped to 8074.5 μs and then followed the trend set by water temperature.

Evidently the cleaning operation was effective in removing the wall coating. The strongest evidence is the sudden drop in period reading that occurred at 1100 hours on Monday. The data on figure 9 also indicate the tube remained clean for about 20 hours after each cleaning operation. Beyond this time limit, errors increased rapidly.

ERROR-CORRECTING FORMULA

The first step in developing the error-compensation formula is to evaluate sensitivity coefficients for suspended-sediment concentration, dissolved-solids concentration, temperature, depth, and flow velocity. As table 2 shows, each factor is related to one and only one sensitivity coefficient. Shifting the value of the factor causes a shift in vibrational period. Dividing the period shift by the factor shift yields the value of the particular coefficient. Each coefficient is derived from data indexed in the third column of the table.

The sensitivity coefficients can be used to relate period readings for two sets of conditions or <u>states</u>. A state is defined by the vector (set of readings) S_n, D_n, T_n, W_n, V_n, and P_n. The first five symbols are defined in the first column of table 2: the sixth symbol, P, designates vibrational period. The subscript "n" designates state number and takes on the value of either 1 or 2. For example, P_1 designates vibrational period for state 1 and T_2 designates temperature for state 2.

Let us consider a special case in which state 1 and state 2 differ but only with respect to sediment concentration and vibrational period. Figure 3 (quartz-suspension line) shows that the two states are related as follows:

$$P_2 = P_1 + 0.0013(S_2 - S_1). \qquad (1)$$

The last term in this equation is the shift in period caused by the shift in sediment-concentration in going from S_1 to S_2.

Table 2.--*Summary of sensitivity coefficients*

[μs, microsecond; °C, degrees Celsius; mg/L, milligram per liter; m, meter]

Factor and symbol	Sensitivity coefficient	Source of data
Suspended-sediment concentration, S	0.0013 μs/(mg/L)	fig. 3, quartz-suspension line
Dissolved-solids concentration, D	0.0016 μs/(mg/L)	fig. 3 sodium-chloride line
Temperature, T	1.97 μs/°C	fig. 10
Depth, W	1.0 μs/m	fig. 11
Flow velocity, V	0.075 μs/(m/S)	fig. 14

In general, state 1 and state 2 differ with respect to all factors listed in table 2. Extending the pattern in equation 1 to include the entire list, we obtain

$$P_2 = P_1 + 0.0013(S_2 - S_1) + 0.0016(D_2 - D_1) + 1.97(T_2 - T_1) + 1.0(W_2 - W_1) + 0.075(V_2 - V_1). \quad (2)$$

Solving equation 2 for S_2 and then rounding all coefficients to two significant places we obtain,

$$S_2 = S_1 + 770.(P_2 - P_1) - 1.2(D_2 - D_1) - 1500.(T_2 - T_1) - 770.(W_2 - W_1) - 58.(V_2 - V_1). \quad (3)$$

Equation 3 along with state-1 and state-2 vectors is related to the survey-tape problem discussed in the introduction. The state-2 vector is analogous to a plane with an elevation that is specified relative to a datum. The datum corresponds to the state-1 vector. Viewed from another perspective, the state-2 sediment-concentration, S_2, is obtained by starting with S_1 and then applying correction factors given by the last four terms in equation 3.

By starting with equation 3, we can formulate a procedure for collecting sediment-concentration data. Low-flow conditions will probably afford the most convenient setting for establishing the datum or state-1 vector. First, a water sample must be collected and then analyzed to obtain a value for S_1. The remaining readings are obtained from meters installed at the site: a vibrational-period meter connected to the model-B gage gives P_1; a specific-conductance meter gives a value from which D_1 can be computed; a thermometer gives T_1; a stage reading along with the elevation of the model-B gage gives W_1; last of all, a current meter gives V_1. It is important to collect the water sample and read all meters at about the same time.

After defining the state-1 vector, the next step is to collect a series of state-2 vectors. All readings comprising a single state-2 vector must be collected at about the same time. After logging a state-2 vector the process must be repeated after a chosen time interval. Two minutes is a reasonable interval, but it can range from as short as a few seconds to as long as several hours or even several days.

After several state-2 vectors have been recorded, the data-reduction phase can begin. Each sediment-concentration value is obtained by inserting a set of state-2 readings into equation 3 and then solving for S_2. An example is given in table 3. The top half of the table shows raw data comprising the state-1 and state-2 vectors. The bottom half shows the reduced data and gives a list of S_2 values in the right-hand column.

New state-1 readings should be collected every few weeks to document any permanent changes occurring in vibration rates. Like any sensitive instrument, the sediment gage may suffer from long-term aging of its electrical and mechanical components. For example, gradual weakening of the permanent magnets may cause slow, irreversible shifts in the period readings. The gage may also react to mechanical shocks if they are severe enough to disturb alignment of the tube, magnets, or coils.

The procedures for implementing equation 3 must, at this time, be viewed as a plan that has been only partially verified by field tests. The diversion-channel test is the only experiment that was run under simulated field conditions. The test yielded a large body of data; however, the readings are not suitable for a test case because the flow contained sediment at a concentration of only 12 mg/L--a level well below the gage's detectable limit. The Willow Creek test data were, on the other hand, corrected by using a method similar to the one described in this section. The major difference was that a correction factor for depth was not applied since the U-tube gage was mounted on the shore.

UNCERTAINTIES AND LIMITATIONS IN SEDIMENT-CONCENTRATION READINGS

Readings from the gage can be transformed to sediment-concentration values, but the transformation involves a certain degree of uncertainty (inaccuracy). This in turn limits the gage's range of application. Figure 10, shows scatter in the data and the relation of this scatter to precision in sediment-concentration values. Randomness in the period readings sets a level of uncertainty in obtaining sediment concentrations. The "probable error," a common means of expressing this uncertainty, is graphically shown by the shaded area (fig. 10) that straddles the regression line and covers 6 of the 13 plotted points. The height of the band projected onto the period scale is about $\pm$ 0.3 μs. This indicates that even if temperature is perfectly stable, period reading will fluctuate. Out of a large number of period readings, about half will differ from the mean by less than 0.3 μs. The slope of the quartz-suspension line on figure 3 indicates that a $\pm$ 0.3 μs change in period corresponds to a $\pm$ 230 mg/L shift in sediment concentration.

Table 3.--*Example of data-reduction procedure*

S--Suspended sediment concentration, milligrams per liter

p--Vibrational period, in microseconds

K--Specific conductance, in microsiemens per centimeter

T--Temperature, in degrees Celsius

W--Depth, in meters

V--Flow velocity, in meters per second

D--Dissolved-solids concentration, in milligrams per liter

Subscripts 1 and 2 refer to States 1 and 2, respectively

Raw Data State-1

S_1, mg/L	P_1, μs	K_1, μS/cm	T_1, °C	W_1, m	V_1, m/s	D_1,(1) mg/L
200	7902.3	210	21.1	0.50	0.60	112.

Raw Data State-2

Time, hours	P_2	K_2	T_2	W_2	V_2	D_2(1)
1030	7908.0	170	21.0	0.72	0.80	91.
1040	7908.3	170	21.0	0.70	0.80	91.
1050	7910.5	165	20.8	0.75	0.78	88.
1100	7923.1	150	20.7	0.75	0.72	80.
1110	7925.1	120	20.5	0.80	0.75	65.
1120	7930.2	100	20.5	0.72	0.60	54.
1130	7928.4	96	20.1	0.69	0.60	52.
1140	7919.2	90	19.9	0.61	0.60	49.

Reduced Data State-2

Time, hours	$P_2 - P_1$, μs	$D_2 - D_1$, mg/L	$T_2 - T_1$, °C	$W_2 - W_1$, m	$V_2 - V_1$, m/s	S_2,(2) mg/L
1030	5.7	-21	-0.1	0.22	0.20	4600
1040	6.0	-21	-0.1	0.20	0.20	4800
1050	8.2	-24	-0.3	0.25	0.18	6800
1100	20.8	-32	-0.4	0.25	0.12	17000
1110	22.8	-47	-0.6	0.30	0.15	18000
1120	27.9	-58	-0.6	0.22	0.00	22000
1130	26.1	-60	-1.0	0.19	0.00	22000
1140	16.9	-63	-1.2	0.11	0.00	15000

(1) $D = 2.3 + 0.52K$ where D is dissolved-solids concentration in mg/L and K is specific conductance in μS/cm. This relation, which was developed for the Willow Creek gaging station near Madison, Wisconsin, will not apply to all stations.

(2) Obtained by inserting the terms (P_2-P_1) ... (V_2-V_1) into equation 3 and rounding the result to two significant decimal places. For example at 1050 hours: $S_2 = 200. + 770.(8.2) - 1.2(-24.) - 1500.(-0.3) - 770.(0.25) - 58.(0.18) = 6800.$

Another source of uncertainty stems from the gage's response to temperature shifts and our inability to measure these shifts precisely. As temperatures rise and fall, period readings increase and decrease according to the relation given by the solid line in figure 10. If a 0.1 °C shift in temperature escapes detection, a 150 mg/L error appears in the computed sediment concentration. Systematic errors of this type can be minimized by using an accurate thermometer; however, the errors can never be completely eliminated.

Systematic and random errors occur not only in temperature but in all of the factors appearing on the right side of equation 3. Functioning in concert with one another, these errors will limit the gage to monitoring sediment concentrations greater than a certain threshold, the value of which is estimated at about 1,000 mg/L. The significance of the 1,000 mg/L threshold can be assessed by examining figure 15, a scatter diagram of sediment data from 210 daily stations in the United States (Skinner and Beverage, 1976). Each station is characterized by a single point plotted opposite a C_9 value and a C_{99} value. The C_9 value is approximately equal to the station's minimum sediment concentration, which usually occurred during low-flow conditions. The C_{99} value is approximately equal to the station's maximum sediment concentration, which usually occurred during brief, high-flow events. Figure 15 shows that about half of the stations had C_{99} values exceeding 1,000 mg/L, but only one station had a C_9 value exceeding 1,000 mg/L.

The high threshold value for the gage will limit potential applications to monitoring peak-flow, high-concentration events. Since these events are of short duration, it may be necessary to operate the model-B gage alongside an automatic pumping sampler. The concentration of pumped samples can serve as calibration points for data collected with the model-B.

FUTURE TESTING AND DEVELOPMENT

In its present form, the model-B gage can be used only at field sites that meet requirements for high sediment concentrations. The scope of application would be much broader if two sources of interference--temperature and depth--could be reduced or eliminated entirely.

Temperature affects every component in the gage, but the influence is most strongly felt by the vibrating tube itself. Warming produces dimensional dilations proportional to the coefficient of thermal expansion, which for the stainless-steel tube in the model-B is about 17.0 $\mu m/m/°C$. Substituting a material with a smaller coefficient may improve performance, but the choice of substances is limited. Hastelloy, one of the exotic commercial alloys with excellent mechanical and chemical properties, has a thermal coefficient of 11. Tungsten and zirconium, elements even more stable than Hastelloy, have a coefficient of 5. Materials with even smaller coefficients fall in the category of ceramics and glasses. For example, high-quality silica has a coefficient of 0.8; fused quartz has a coefficient of 0.5. One or both of these substances may serve as a possible substitute for stainless steel.

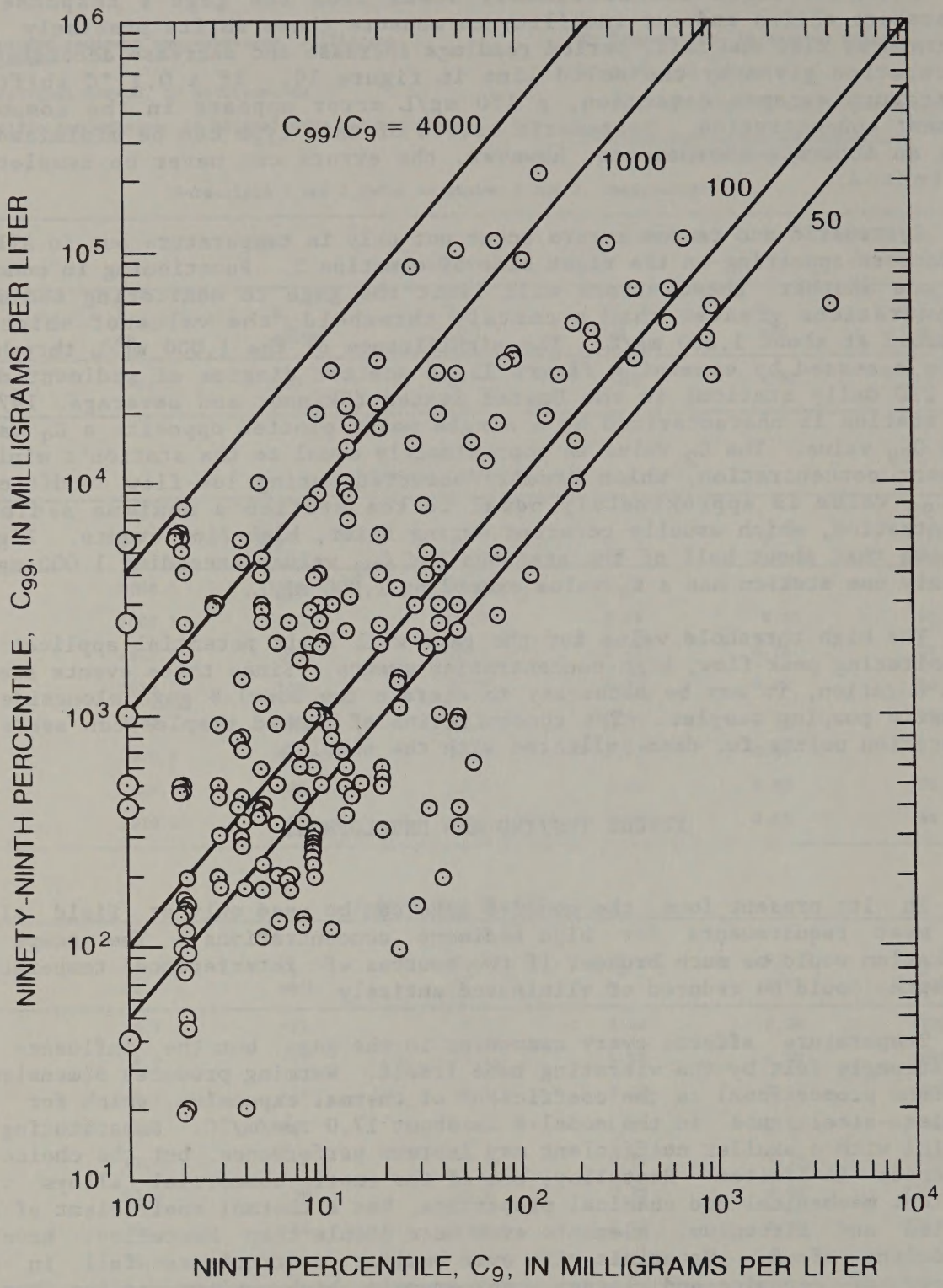

Figure 15.--Distribution of C_9 and C_{99} values for 210 daily sediment stations monitored during 1967.

Water depth is an interference that may actually be masking another, more basic effect--vibration of the sleeve that supports the ends of the tube. During the design phase, inertia was believed to be adequate for suppressing vibration of the sleeve; consequently, this part was purposely made several hundred times heavier than the tube. During the testing phase, certain conditions led to surprising and somewhat disappointing results. The sleeve sometimes resonated with the surrounding water, and when this happened the reverberations amplified the motion of the sleeve and shifted the tube's frequency. The addition of vibration dampers may eliminate these resonant conditions. The dampers, which consist of tuned, spring-mass combinations, are commonly used to suppress vibration of unbalanced, rotating machines. The dampers can be bolted inside the sleeve so they can operate without interfering with water flow or sediment movement outside the gage.

SUMMARY

The model-B gage consists of a submersible, streamlined shell that supports a slender tube. The tube vibrates continuously at a rate governed not only by the concentration of sediment inside the tube but also by the temperature of water in the tube, the depth of the tube below the water surface, the flow velocity of water moving through the tube, and the concentration of dissolved solids in the water. The last four factors introduce errors in the sediment-concentration measurements; however, the errors can be minimized with the aid of a simple formula. The formula contains one term for each error factor. All coefficients in the formula are constants.

Although the formula is useful, it is deficient in one respect. It does not correct errors caused by the accumulation of debris on the walls of the tube. The only way to minimize these errors is through periodic cleaning.

In its present form, the gage will work best at sites where concentrations exceed 1,000 mg/L most of the time. Additional development work aimed at stabilizing the tube's thermal response and reducing the sleeves vibratory motion will probably reduce the detection limit and extend the instruments range of application.

REFERENCES CITED

Beverage, J. P., 1982, A fluid-density gage for measuring suspended-sediment concentration, Part B in Report X of A study of methods used in measurement and analysis of sediment loads in streams: Minneapolis, Minn., Interagency Advisory Committee on Water Data, Federal Interagency Sedimentation Project, 125 p.

Bird, L. L., Papadopoulos, J., Rex, R. A., and Ziegler, C. A., 1963, Radiological mechanisms for geophysical research: AEC Research and Development Report NYO 10,220, Parametrics Inc., Waltham, Mass., 61 p.

Housner, G. W., 1952, Bending vibrations of a pipe line containing flowing fluid: Journal of Applied Mechanics, no. 19, p. 205-208.

Interagency Committee on Water Resources, Subcommittee on Sedimentation, 1963, Determination of fluvial sediment discharge, Report 14 of A study of methods used in measurement and analysis of sediment loads in streams: Minneapolis, Minn., Federal Interagency Sedimentation Project, 151 p.

----- 1941, Laboratory investigation of suspended sediment samplers: Report 4, 99 p.

National handbook of recommended methods for water-data acquisition, 1977, Office of Water-Data Coordination: U.S. Geological Survey, chap. 3-Sediment, p. 9.

Skinner, J. V., 1982, A fluid-density gage for measuring suspended-sediment concentration, Part A in Report X of A study of methods used in measurement and analysis of sediment load in streams: Minneapolis, Minn., Interagency Advisory Comm. on Water Data, Federal Interagency Sedimentation Project, 125 p.

Skinner, J. V. and Beverage, J. P., 1976, Instrumentation - Automatic collection of sediment data, in Proc. of Third Federal Interagency Sedimentation Conference, Sedimentation Committee, Water Resources Council, Denver, Colo., Symposium 7, p. 1-15.

Skinner, J. V., Beverage, J. P., and Goddard, L. L., 1986, Continuous Measurement of Suspended Sediment Concentration; Proceedings of the Fourth Federal Interagency Sedimentation Conference, Subcommittee on Sedimentation, v. 1, p. 29-39.

Szalona, J. J., 1986, Progress report: Description and test of a straight tube fluid-density gage for measuring suspended-sediment concentration in streams, Report HH of A study of methods used in measurement and analysis of sediment loads in streams: Minneapolis, Minn., Interagency Advisory Comm. on Water Data, Federal Interagency Sedimentation Project, 29 p.

Vanoni, V. A. (ed.), Am. Soc. Civil Engineers, 1975, Sedimentation engineering: Manual on Engineering Practice no. 54: New York, p. 22.